The Haar Wavelets used how Expansion Function in the Method of the Moments in the Solution of Some Electrostatic Problems

Aldo Artur Belardi
Electrical Department
Centro Universitário da FEI
Av. Humberto de Alencar Castelo Branco, n° 3972, 09850-901, São Bernardo do Campo
belardi@fei.edu.br
José Roberto Cardoso & Carlos A. França Sartori
Electrical Department
Escola Politécnica da Universidade de São Paulo
Av. Prof. Luciano Gualberto, travessa 3, n° 158, 05508-900, São Paulo. Brazil
cardoso@pea.usp.br & sartori@pea.usp.br

Abstract: - This work presents the methodology from the determination the charge superficial density and electrical fields, in three simple structures to a finite straight wire, square plane plates and the capacitance between to plane plate, all finite and submitted to a constant potential. That involves the method of the moments using as expansion function the Haar wavelets instead of the pulse function, in order to reach a good precision and reducing the computational execution time. We also intend to take advantages of the wavelets application through the Cholesky decomposition, talking about formation of scattered matrixes, and the detection of nulls values.

Key-Words: - Moments, Wavelets, Electrostatic

1 Introduction

1.1 Method of Moments

The method of moments is a general method based on weighted waste [1][2]. This method includes many specific methods known can be mentioned the method of simulation of load, the method of finite elements, which are considered as one of the special cases of the method of moments.

Any method, in which a system matrix can determine the coefficients of an equation, can be interpreted as a variation of the method of moments.

Thus, the steps for applying the method of moments can be systematized as follows:

a) Select a function to replace the approximate unknown function;

b) Select a function of expansion and weighting;

c) Completing the internal product between the function of expansion and weighting to obtain the resulting matrix;

d) Solution of matrix equation using a computer program to obtain the approximate solution.

The basis of the method of moments approach is a function of the type:

$$f(x)=\sum_n \alpha_n \boldsymbol{L} g_n \qquad (1)$$

Where α_n are constants not known, g_n is a function of expansion and $\boldsymbol{L}$ is a mathematical operator.

Becoming the internal product with a function Wm weight we get in matrix form:

$$A=\begin{bmatrix} <\boldsymbol{L}g_1, W_1> & <\boldsymbol{L}g_2, W_1> ..... <\boldsymbol{L}g_n, W_1> \\ <\boldsymbol{L}g_1, W_2> & <\boldsymbol{L}g_2, W_2> .... <\boldsymbol{L}g_n, W_2> \\ : & : & : \\ <\boldsymbol{L}g_1, W_n> & <\boldsymbol{L}g_2, W_n> ..... <\boldsymbol{L}g_n, W_n> \end{bmatrix}$$

$$B=\begin{bmatrix} <f, W_1> \\ <f, W_2> \\ : \\ <f, W_n> \end{bmatrix} \qquad (2)$$

that is A[α]=B, where[α] is the composed column of vectors for the unknown coefficients of the approach solution. In such a way if the properties of the adopted function, coincide with the properties of the accurate solution, then the approach solution will go to converge quickly.

Some additional factors such as accuracy in the solution, ease of solution of the resulting matrix, the

size of the array etc, depend on the choice of basis function and weighting function.

When we adopted the function of weight equal to the basic function, the result obtained in the method of moments is called the method of Galerkin.

Making up the domestic product with a weighting function and using the matrix notation, we have that [A]*[α]=[B], being [α] a column vector composed of unknown coefficients of the approximate solution.

1.2 Wavelets

Many scientists already used analysis of wavelets as an alternative to classical Fourier analysis of [3][4][5]. In the last ten years, the interest in wavelets has grown tremendously since 1985, when he was given a new impetus to this theory through the contributions of mathematicians and specialists in signal processing. In general, the wavelet can be defined by:

$$\psi_{a,b}(x) = |a|^{-1/2}\,\psi\left(\frac{x-b}{a}\right) \quad a,b \in R, a \neq 0 \qquad (3)$$

The function Ψ is called mother wavelet, the values of (a) and (b) defined by $a=2^{-j}$ and $b=k2^{-j}$ with j and k belonging to the set of whole numbers on.

Some types of wavelets mentioned in literature exist, being that the use of a type or another one directly is associated with the application. Rules of construction are being proposals for some researchers in accordance with the restrictions and necessities of each case.

We can generate infinity of wavelets different and particularly to construct a set adjusted for processing of signals, specific expanses, obtaining with this the attainment of better resulted.

Beyond wavelet of presented Haar previously we show to some wavelets such as Morlet, Hat Mexican and Shannon.

The Fig. 1 we represent wavelet of Morlet, or modulated Gaussian that is formulated by:

$$\psi(x) = e^{i\omega_0 x} e^{-x^2/2} \qquad (4)$$

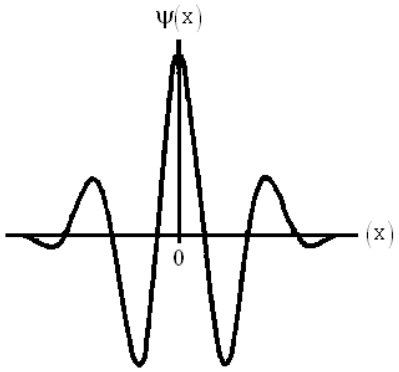

Fig. 1 - Morlet wavelet

The Fig. 2 we represent Mexican hat wavelet that is formulated by:

$$\psi(x) = (1-x^2)e^{-x^2/2} \qquad (5)$$

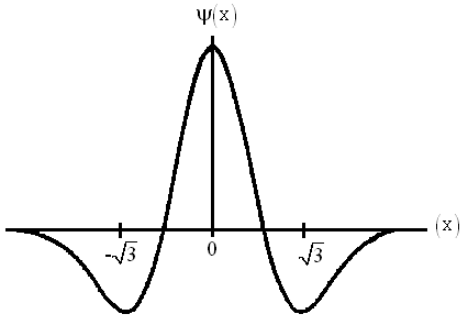

Fig.2 - Mexican hat wavelet

The Fig. 3 we represent Shannon wavelet that is formulated by:

$$\psi(x) = \frac{\sin(\frac{\pi x}{2})}{\frac{\pi x}{2}}\cos(\frac{3\pi x}{2}) \qquad (6)$$

$$\varphi(x) = \begin{cases} \dfrac{\sin(\pi x)}{\pi x}, & x \neq 0 \\ 1, & x = 0 \end{cases}$$

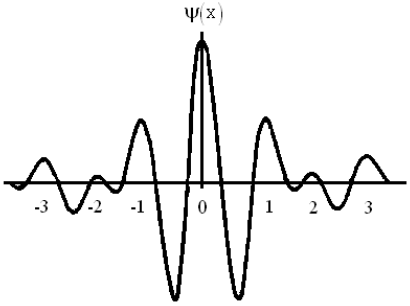

Fig. 3 - Shannon wavelet

1.2.1) One-Dimensional wavelets

Considering the space $L^2(R)$, of all measurable functions of square integrated over R, and considering it is an orthogonal basis generated by Ψ, for any f(x) of square integrated on R we have[6][7][8]:

$$f(x) = \sum_{j=-\infty}^{\infty} \sum_{k=-\infty}^{\infty} c_{j,k} \psi_{j,k}(x) \qquad (7)$$

An example of wavelet is the Haar function of which is defined as Fig. 4:

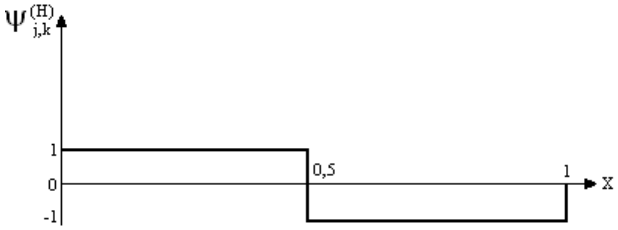

Fig.4 - Haar function

The Haar wavelet is defined by the two families of wavelet, the mother and father, the latter being represented by ϕ a scalar function defined by [4]:

$$\phi^{(H)}(x) = \begin{cases} 1 & 0 \le x < 1 \\ 0 & \text{other case} \end{cases} \qquad (8)$$

The Fig. 5 shows graphically the intervals and amplitudes for the Haar wavelet one-dimensional, until the level two of resolution, representing the amplitude of the function obtained by varying the level j and the displacement of k.

The set of wavelets coefficients obtained with the contribution of each will be used to determine the function f(x,y) at each point.:

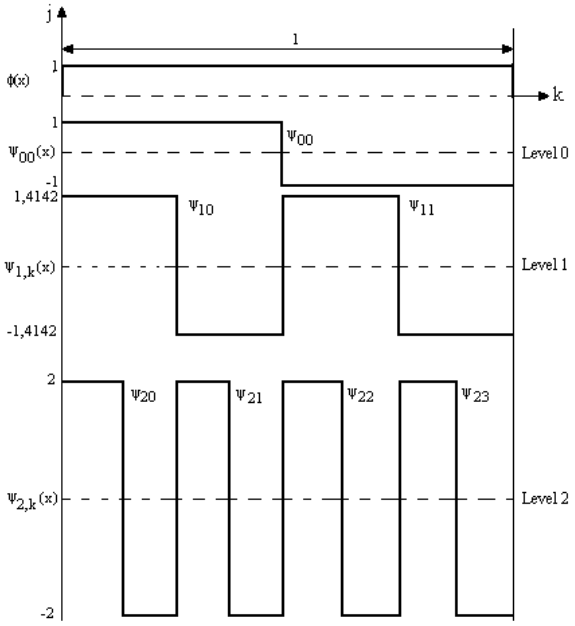

Fig.5 - The Haar function one-dimensional until level two of resolution.

Considering the mother wavelets and father, the function f (x) can be written by:

$$f(x) = \sum_{k=-\infty}^{\infty} c_{0,k} \phi^{(H)}(x) + \sum_{j=-\infty}^{\infty} \sum_{k=-\infty}^{\infty} c_{j,k} \psi_{j,k}^{(H)}(x) \qquad (9)$$

1.2.2) Two-dimensional wavelets

We can build databases of two-dimensional wavelet, through a base in two dimensions with a single scale, or also by two bases of a size, with separate scales for each dimension [9]. Another possibility is to work with the mix of products between each of the two axes with different scales for each dimension [10][11][12]. Thus for any point P, until the level 1 resolution will:

$$\psi_{j,k}^{(H)}(x) = \begin{bmatrix} \phi(x) & \psi(x) & \psi(2x) & \psi(2x-1) \\ \psi(4x) & \ldots & \psi\left(2^j x - k\right) & \end{bmatrix} \qquad (10)$$

$$\psi_{j,k}^{(H)}(y)=\begin{bmatrix}\phi(y)\ \psi(y)\ \psi(2y)\ \psi(2y-1)\\ \psi(4y)\ldots\psi\left(2^{j}y-k\right)\end{bmatrix} \quad (11)$$

for a point P any until resolution level 1 we will have

$$\psi^{(H)}(x)=\left[\phi(x)\ \psi(x)\ \psi(2x)\ \psi(2x-1)\right] \quad (12)$$

$$\psi^{(H)}(y)=\left[\phi(y)\ \psi(y)\ \psi(2y)\ \psi(2y-1)\right] \quad (13)$$

For each axis, x is given by $\psi^{(H)}(x)$ an y is given by $\psi^{(H)}(y)$, resulting in the following contributions:

$$\begin{aligned}&\phi(x)\phi(y),\phi(x)\psi(y),\phi(x)\psi(2y),\\&\phi(x)\psi(2y-1),\ldots,\psi(2x-1)\psi(2y-1)\end{aligned} \quad (14)$$

The Fig.6 shows the decomposition of the amplitude and the scale for wavelet of Haar for two dimensions until resolution level 1, for any point P.

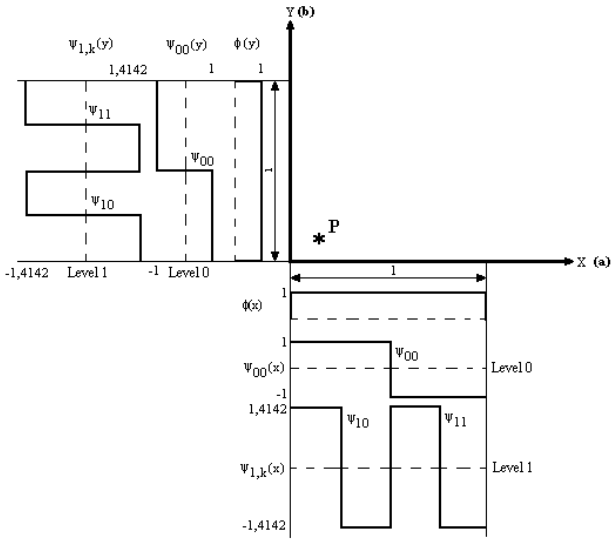

Fig. 6 - The Haar function two-dimensional

2 Mathematical developments

Here, we present the mathematical development for the application of the method of moments in determining the surface charge density for a finite straight wire (one-dimensional case) and a square plane plate (two-dimensional case), and capacitance square plane plate, all subjected to a constant potential.

2.1 One-dimensional case

First, Fig.7 we conducted a study of the distribution of electric charges in a finite straight wire with diameter (0.0001mm), resulting in an equation of a variable of type [13]:

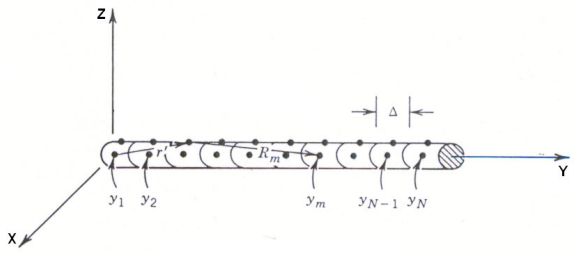

Fig. 7 - Subdivision of a finite straight wire

$$V(r)=\frac{1}{4\pi\varepsilon}\int\frac{\rho(r')}{R(r,r')}dl' \quad (15)$$

As the wire is straight and finite and positioned in the x axis, the observations in relation to axes y and z are considered equal to zero. The electrostatic potential is written by:

$$\begin{aligned}&V(x,y\text{ and }z=0)=V(r)\\&V(r)=\frac{1}{4\pi\varepsilon}\int\frac{\rho(r')}{R(x,x')}dl'\end{aligned} \quad (16)$$

To calculate the potential and other physical quantities such as capacitance, electric field, etc., we calculate the surface density, which is an unknown quantity, which is within a mathematical operator.

The determination of linear density of charge can be approximated by expansion in N terms, composed by the sum of coefficients multiplied by the function of expansion and weighting. Dividing the wire into N equal segments, we have the length of each part worth Δ=L/N.

Applying the weighting function as $W_m=\delta(x-x_m)=1$, the internal product at point is given by:

$$V(r)_{Point} = \delta(x-x_m)\times \times\frac{1}{4\pi\varepsilon}\sum_{n-1}^{N}\alpha_n\int_0^L\frac{g_n(x')}{\sqrt{(x-x')^2+a^2}}dx' \quad (17)$$

Assuming that the load obtained in each subdivision of the wire is positioned in the center of gravity of each division, replacing it if the value of x by the distance of the load considered in relation to that, we have an integral that is only function of x'.

Using the matrix notation, each Z_{mn} is defined by:

$$Z_{mn} = \int_0^L \frac{g_n(x')}{\sqrt{(x_m-x')^2+a^2}}dx' \quad (18)$$

2.2 Two-dimensional case

Through the methodology presented above, the potential in a finite plane plate with very fine thickness creates a potential given by[14]:

$$V(x,y) = \frac{1}{4\pi\varepsilon}\int_{-a}^{a}dx'\int_{-b}^{b}\frac{\rho(x',y')}{\sqrt{(x-x')^2+(y-y')^2}}dy' \quad (19)$$

The Fig 8 showed dividing each of the lines into segments equal and assuming that the distribution of load is concentrated in the center of gravity of each area ΔS_n, the influence of the load at the position (x,y), on the other determined by the coordinates (x',y'), R is defined by the distance between loads.

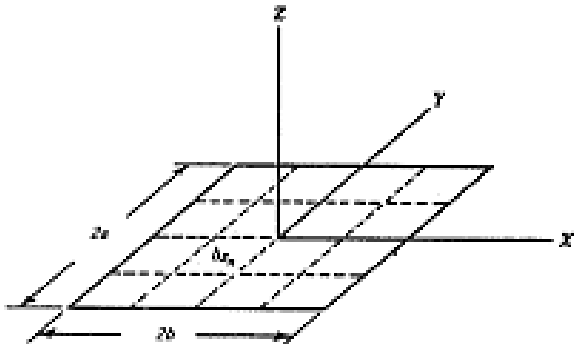

Fig. 8 - Subdivision in a plain plate

Applying the method of moments, the distribution of load can be approximated by the following equation:

$$V(x,y)_{Point} = \langle W_m, f, \boldsymbol{L}g\rangle = \delta(x-x_m)\delta(y-y_m)\times \times\frac{1}{4\pi\varepsilon}\int_{-a}^{a}dx'\int_{-b}^{b}\frac{\sum_{n=1}^{N}\alpha_n g_n(x',y')}{\sqrt{(x-x')^2+(y-y')^2}}dy' \quad (20)$$

Replace the value of x e y by the distance R, for the each point x_m and y_m, we have an integral function of which is only x' and y'.

$$Z_{mn} = \int_{-a}^{a}dx'\int_{-b}^{b}\frac{g_n(x',y')}{4\pi\varepsilon\sqrt{(x_m-x')^2+(y_m-y')^2}}dy' \quad (21)$$

2.3 The capacitance calculation

The capacitance of a unit square plate can be evaluated based on the following well-known expression [15]:

$$C = \frac{q}{V} = \frac{1}{V}\int_{-a}^{a}\int_{-b}^{b}\sigma(x,y)\,dxdy \quad (22)$$

If a square parallel conducting plane plates is considered as an example, we should remember that the potential in a finite and very thin plane plate can be evaluated by:

$$V(x,y,z=0) = \frac{1}{4\pi\varepsilon}\times \times\int_{-a}^{a}dx'\int_{-b}^{b}dy'\frac{\sigma(x',y')}{[(x-x')^2+(y-y')^2+d^2]^{1/2}} \quad (23)$$

Thus, after applying the method of the moments, knowing the function of the approximated solution f(x,y), the expansion function g(x,y) and the weighed function W(x,y) and d the distance between the parallel square plates, the potential in a square plane plate, will be estimated by the inner product of these functions:

$$V(x,y)=\langle g,W,f\rangle\frac{1}{R}= \\ =\int_{-a}^{a}\int_{-b}^{b}\frac{g(x,y)W(x,y)f(x,y)}{R(x,y)}dxdy \quad (24)$$

Dividing the plate in equal segments and applying the weighed function as being the delta function of Dirac, we had that $W_m=\delta(x-x_m)\ \delta(y-y_m)$, being the inner product in the point given by:

$$V(x,y,z=0)=\delta\left(x-x_m\right)\delta\left(y-y_m\right)\times \\ \times\frac{1}{4\pi\varepsilon}\int_{-a}^{a}dx'\int_{-b}^{b}dy'\frac{\sum_{n=1}^{N}\alpha_n g_n(x',y')}{[(x_m-x')^2+(y_m-y')^2+d^2]^{1/2}} \quad (25)$$

When two parallel plates are considered, the calculation of the plate capacitance, submitted to voltage +V on the top plate and –V on the bottom plate, can be evaluated by:

$$C=4a^2\sum_{mn}\left(l^{tt}-l^{tb}\right)^{-1}_{mn} \quad (26)$$

where t denotes "top plate" , b denotes "bottom plate", and l is a matrix which elements depend on the plate charge contributions.

Assuming the charges placed in the centre of each sub division in relation to each axes, substituting the values of x and y by the distance of the charge position to the point $P(x_m,y_m)$, for a fixed potential V, the equation can be represented, by matrix notation, Z_{mn} is defined by:

$$Z_{mn}=\int_{-a}^{a}dx'\int_{-b}^{b}\frac{g_n(x',y')}{4\pi\varepsilon\sqrt{(x_m-x')^2+(y_m-y')^2+d^2}}dy' \quad (27)$$

3 Applications

3.1 Application one-dimensional

To verify the performance of wavelets in the method of moments, we conducted a study on a finite straight wire. In this case, is used as basis for expansion of the Haar wavelet function and the weighting of the Dirac Delta function [16].

The potential in a finite straight wire, can be written by:

$$V(r)=\frac{1}{4\pi\varepsilon}\left[\int_0^L\frac{c_0\phi(x)}{R(x,x')}dx+\int_0^L\frac{\sum_{n=1}^{N}c_{j,k}\psi_{j,k}^{(H)}(x')}{R(x,x')}dx\right] \quad (28)$$

We split the wire with a length of 1m and diameter of 0.0001m, into eight equal segments according to Fig. 9.

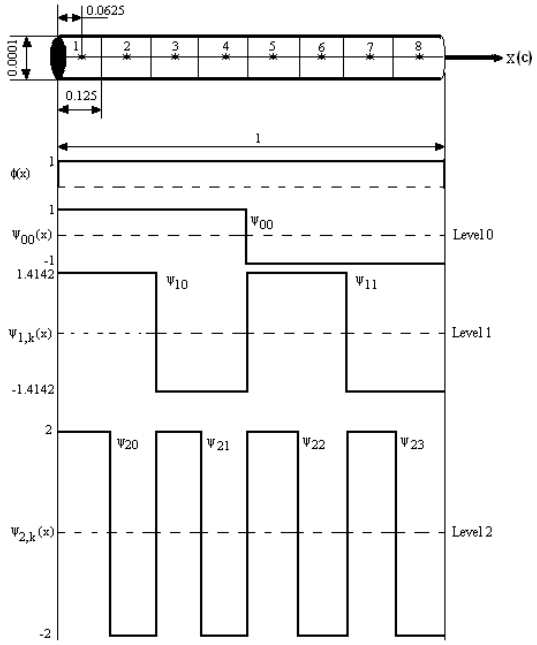

Fig. 9 - Contribution of each level in the the number of subdivisions

For the first point, considering all the subdivisions, we have:

$$Point_1=c_0\int_0^L\frac{1}{\sqrt{(x_m-x')^2+a^2}}dx+ \\ +c_{00}\int_0^{\Delta}\frac{1}{\sqrt{(x_m-x')^2+a^2}}dx+ \\ +c_{10}\int_0^{\Delta}\frac{\sqrt{2}}{\sqrt{(x_m-x')^2+a^2}}dx+ \\ +c_{20}\int_0^{\Delta}\frac{2}{\sqrt{(x_m-x')^2+a^2}}dx \quad (29)$$

Solving the integral and is based on x_m with the distance of the load source to source, we must each Z_{mn} is defined by:

$$Z_{mn} = \ln \frac{n\Delta - x_m + A}{n\Delta - \Delta - x_m + B}$$
$$A = \sqrt{(x_m^2 - 2x_m n\Delta + a^2 + n^2\Delta^2)} \quad (30)$$
$$B = \sqrt{(x_m^2 - 2x_m n\Delta + 2x_m\Delta + a^2 + n^2\Delta^2 - 2\Delta^2 n + \Delta^2)}$$

The calculation of linear density of charge at each point, using as a basis for expansion of the Haar wavelet, is given by:

$$\rho(x)_{Point\,P} = c_0\phi(x) + c_{00}\psi_{00}(x) + \\ + c_{10}\psi_{10}(x) + ... + c_{jk}\psi_{jk}(x) \quad (31)$$

The Table I present the results of the linear density of charge for a straight wire with a length of 1.0 m, divided into 16 equal segments, depending on the level of resolution (j) and the displacement (k).

Table I - Value of the linear charge density (pc/ m) of a finite straight wire in terms of levels of resolution.

	Expansion Function			
Point	Haar wavelet (Level)			Pulse
	2	3	4	
1	8.835	9.376	9.957	9.957
2	8.835	9.376	8.764	8.764
3	8.835	8.274	8.411	8.411
4	8.835	8.274	8.219	8.219
	7.970	8.059	8.102	8.102
…	…	…	…	…
12	7.970	8.059	8.102	8.102
13	8.835	8.274	8.219	8.219
14	8.835	8.274	8.411	8.411
15	8.835	9.376	8.764	8.764
16	8.835	9.376	9.957	9.957

The Fig. 10 presents the load distribution when the wire is divided 32 equal segments, submitted to a constant potential of 1V, and using as expansion function wavelet of Haar.

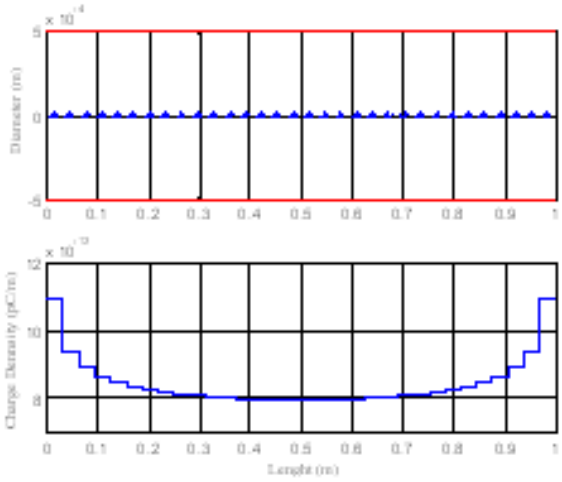

Fig.10 - The surface charge (pC/m) on a 1.0 m straight wire, for 32 subdivisions

3.2 Test of hypothesis for a wire with 32 division using the Haar wavelet and the pulse

We can compare the results gotten between the two numerical methods considering it expansion function as being the pulse with the other using wavelets, through tests on the difference of the pair upped data or between the correlated population averages. We can carry through tests of comparison of averages for pair upped data, when the results of the two samples are related two the two, in accordance with some criterion that supplies an influence between some pairs and on the values of each pair. Thus, we calculate the differences for each pair of values, taking itself in consideration the values of the superficial load density in the point for each one of the numerical methods [17].

Considering it existence hypothesis and the alternative hypothesis, we will have:

$$\text{existence hypothesis} \Rightarrow H_0 : \mu_1 - \mu_2 = \mu_d = 0$$
$$\text{alternative hypothesis} \Rightarrow \mu_d \neq 0 \quad (32)$$

being in majority of cases $\mu_d = 0$, what it means that we will be testing the equality between the averages, that is $H_0 : \mu_1 = \mu_2$, given for:

$$\bar{d} = \frac{1}{n}\sum_{i=1}^{n} d_i \begin{cases} \bar{d} & \Rightarrow \text{measured of sample the differences} \\ d_i & \Rightarrow \text{difference of the surface density in the point} \\ n & \Rightarrow \text{great the sample} \end{cases} \quad (33)$$

the standard of the samples of the differences (s_d) and the estimate of the error standard $s_{\bar{d}}$ are given by:

$$s_d = \sqrt{\frac{1}{n-1}\left\{\sum_{i=1}^{n} d_i^2 - \frac{\left(\sum_{i=1}^{n} d_i\right)^2}{n}\right\}} \Rightarrow s_{\bar{d}} = \frac{s_d^2}{\sqrt{n}} \quad (34)$$

The criterion for comparison between the two methods is given by:

$$Z_{calc} = \frac{\bar{d} - \mu_d}{s_{\bar{d}}} \quad (35)$$

Considering it normal distribution and fixing a level α, we define the regions of not rejection and rejection of H_0.

If $|Z_{calc}|>Z_\alpha$ significant difference between the methods exists and in case $-Z_\alpha<Z_{calc}<Z_\alpha$ that significant difference between the two methods does not exist.

Statistical to verify the validity of the two used methods, in Table II meet some of the gotten results of the superficial load density, for a wire with 32 divisions, using itself as expansion function wavelet of Haar comparatively with the function type pulse, calculating itself it changeable criterion.

Therefore the criterion for comparison between the two methods results in $Z_{calc} = -0.214783$.

Considering it table of the normal distribution and the level of 5% risk, for the alternative hypothesis, $\mu_d \neq 0$, we will have that $-Z_\alpha=Z_\alpha=2.5\%$

Table II - Calculation of the criterion for a wire with 32 divisions using as expansion function wavelet of Haar and the pulse.

	Expansion Function		Surface difference	
Point	Pulse	Haar Wavelet	$dx10^{-14}$	d^2x10^{-25}
1	0.10948601427928	0.10948601427928	75	5.625
2	0.09351201394360	0.09351201394295	65	4.225
3	0.08900319714776	0.08900319714714	62	3.844
4	0.08642505943355	0.08642505943293	62	3.844
…				
29	0.08642505943188	0.08642505943505	-317	100.489
30	0.08900319714822	0.08900319714822	0	0
31	0.09351201394092	0.09351201394441	-349	121.801
32	0.10948601428081	0.10948601428139	-58	3.364
Total	-	-	-175	644.055

For the table of normal distribution $Z_\alpha=1.96$, therefore inside of the region of not rejection. We can conclude that, statistical, significant difference between the two numerical methods does not exist, inside of the level of considered risk.

Although wavelets are adjusted to analyze stationary processes, the consideration of its specter and its esteem can be useful when we pass to the not stationary case. As example, we can mention the analysis of processing of signals and image that can involve some aspects of estimation as: theorem of the sampling with wavelet of Shannon, probability and statistics using wavelets, etc.

Making use of the statistics we will be able to improve the convergence and the precision of the results, through the choice of the parameters and of techniques as of crossed validation, that allows esteem the error of forecast for a model adjusted to the data, using a part of these data esteem the model and the remain to evaluate if it is adjusted or not.

Therefore, through the statistical estimators as for example: the choice of the threshold, the Bayesiana analysis, the model with stationary errors, the esteem of densities, the covariance, etc., we will be able more esteem a function of adjusted expansion in the solution of the problem in study, with a lesser number of resolution levels, reduction of the order of the involved matrices, beyond a faster convergence, making with that let us have a reduction in the computational costs.

3.3 Application two-dimensional

The treatment of the Haar wavelet is given by the two-dimensional combination of products of the function at the point on each axis, considering their coefficients. The potential of a finite plane plate may be written by:

$$V(x,y)4\pi\varepsilon = a_j b_j \int_{-a}^{a}\int_{-b}^{b} \frac{\phi(x,y)}{\sqrt{(x-x')^2+(y-y')^2}} + \left[\sum_{j=-\infty}^{\infty}\sum_{k=-\infty}^{\infty} a_{j,k}b_{j,k}\int_{-a}^{a}\int_{-b}^{b} \frac{\psi_{j,k}^{(H)}(x,y)}{\sqrt{(x-x')^2+(y-y')^2}}dxdy\right] \quad (36)$$

The plate was divided in steps of 0.25 in both the x axis and the y Fig. 11 shows these divisions based on the level of a resolution.

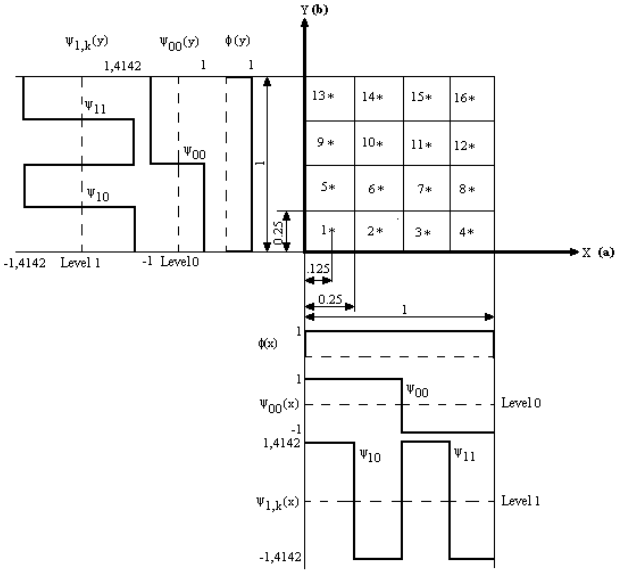

Fig.11 - Contribution of the wavelet on every point made by the subdivision

For the load located in the first subdivision, shall be considered the contributions of the following of Haar wavelets to the level 2 of resolution:

$$\psi_{x1}^{(H)}(x) = \left[\phi(x)\ \ \psi(x)\ \ \psi(2x)\ \ \psi(2x\text{-}1)\right]$$
$$\psi_{y1}^{(H)}(y) = \left[\phi(y)\ \ \psi(y)\ \ \psi(2y)\ \ \psi(2y\text{-}1)\right] \quad (37)$$

Making up the function of weight equal to one and assuming that the density of cargo on a small area ΔS_n is constant, is knowing the value of the potential we can determine the approximate solution, then:

$$m = n \Rightarrow Z_{mn} = \frac{2b}{\pi\varepsilon}\ln\left(1+\sqrt{2}\right) \quad (38)$$

$$m \neq n \Rightarrow Z_{mn} = \frac{\Delta S_n}{4\pi\varepsilon\sqrt{(x_m-x_n)^2+(y_m-y_n)}} \quad (39)$$

The contribution of each wavelet in point will be considered by:

$$EXP_{(P1)} = c_0 + c_1 + \sqrt{2}c_2 + c_4 + c_5 + \sqrt{2}c_6 + \sqrt{2}c_8 + \sqrt{2}c_9 + \sqrt{2}\sqrt{2}c_{10}$$
$$EXP_{(P2)} = c_0 + c_1 + \sqrt{2}c_2 + c_4 + c_5 + \sqrt{2}c_6 - \sqrt{2}c_8 - \sqrt{2}c_9 - \sqrt{2}\sqrt{2}c_{10}$$
$$\bullet$$
$$\bullet$$
$$\bullet \quad (40)$$
$$EXP_{(P16)} = c_0 - c_1 - \sqrt{2}c_3 - c_4 + c_5 + \sqrt{2}c_7 - \sqrt{2}c_{12} + \sqrt{2}c_{13} + \sqrt{2}\sqrt{2}c_{15}$$

The Table III presents the value of some coefficients obtained through the program.

Table III - Value of coefficients using the Haar wavelet of two-dimensional

Coeficientes	Value x 10^{-10}
C_0	0.2903
C_1	**0**
C_2	0.0218
C_3	-0.0218
C_4	**0**
C_5	**0**
:	:
C_{14}	0.0010
C_{15}	-0.0010

The Fig. 12 shows the distribution of load on a square plate, divided into 16 equal segments on each axis, subjected to a constant potential of 1V.

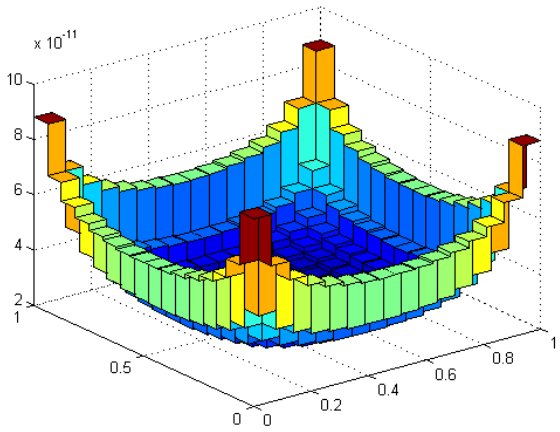

Fig.12 - Distribution of surface charge density on a plane plate divided into 16 equal segments.

3.4 Application capacitance

If the potential in a finite and very thin plane plate is taken into account as an application, it can be evaluated by:

$$V(x,y)4\pi\varepsilon = a_j b_j \int_{-a}^{a}\int_{-b}^{b} (A)\,dxdy + \sum_{j=-\infty}^{\infty}\sum_{k=-\infty}^{\infty} a_{j,k} b_{j,k} \int_{-a}^{a}\int_{-b}^{b} (B)\,dxdy$$

$$A = \frac{\phi(x,y)}{\sqrt{(x_m - x')^2 + (y_m - y')^2 + d^2}} \qquad (41)$$

$$B = \frac{\psi_{j,k}^{(H)}(x,y)}{\sqrt{(x_m - x')^2 + (y_m - y')^2 + d^2}}$$

The Fig. 13 presents the variation of the capacitance between two parallel conducting plane plates as a function of the distance.

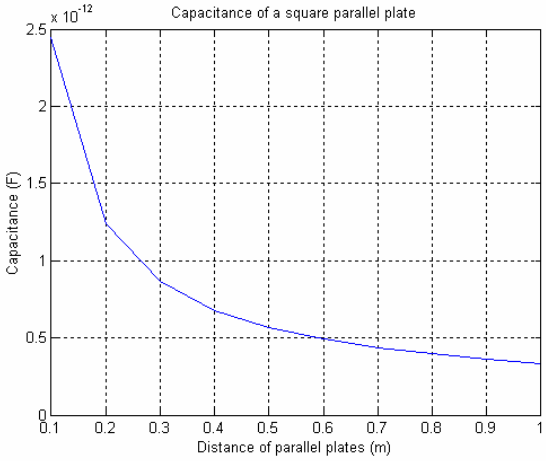

Fig. 13 - Capacitance as a function of the distance

The Table IV presents the comparative results, regarding the computing time values as a function of the number of the axe division, and of the null value detection routine application [18].

Table IV – Computing time (s)

Computing time (s)			
Number of Divisions	Without	With	Difference (%)
4x4	0.1200	0.1000	16.66
8x8	7.7220	4.1260	46.56
16x16	486.990	185.928	61.82

For calculate it of field in the plates we use the sum of the field effect load for load and can be evaluated by:

$$E(r) = \sum_{m=1}^{n} \frac{Q_m}{4\pi\varepsilon |\, r - r_m \,|^2} a_m \qquad (42)$$

The Fig 14 it presents the field that was calculated on each one of square plane plate (1.0mx1.0m), and distance between (0.2m) submitted to a potential of 100 V.

It should be realized that when the null value detection routine is carried out, it will get a 40% average computing time reduction.

After adopting the null value detection routine, an average 40% computing time reduction was achieved.

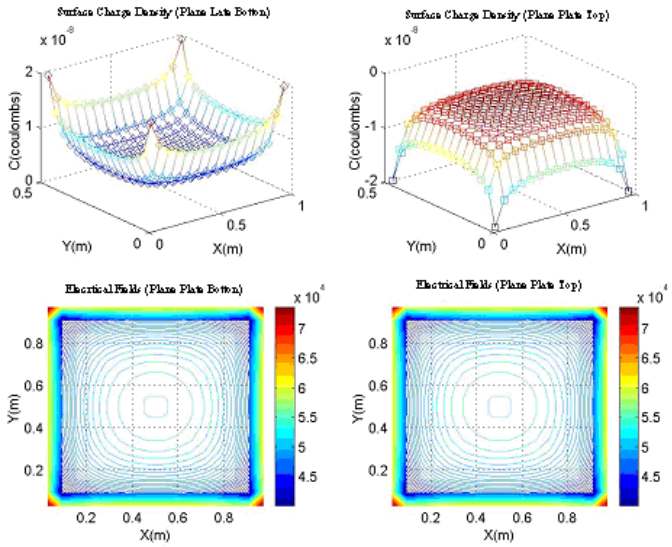

Fig. 14 - Electricals fields square plane plate

4 Computational aspects to plane plate

The application of numerical methods in engineering is to facilitate the solution of complex problems with a response time low. The time of beginning and end of a task is then defined at execution time [19][20]. The performance of a program is defined by:

$$\text{Performance} = \frac{1}{\text{Execution\_time}} \qquad (43)$$

A good number of popular measures can be used in an attempt to create a standard measure of the performance. The result has been simple measurements, valid only in limited contexts. Another popular alternative to measure the execution time is the MFLOPS, or millions of floating point operations per second in, according to:

$$\text{MFLOPS} = \frac{N^0\_\text{operation}\_\text{in}\_\text{floating}\_\text{point}}{\text{Execution\_Time} \times 10^6} \qquad (44)$$

4.1 Measure the performance

In applying a finite plane plate, we measure the time of the program, varying the number of division in each of the axes, measuring both the amount is carried out in floating point operations and the execution time.

The Table V shows the values obtained for the execution time and total number of operations carried out in floating point, using as a basis for expansion of the Haar wavelet.

Table V - Calculation in floating point operations and the execution time according to the number of divisions of the plate

Divisions in each axis	Operations in floating point	Execution time (s)
4X4	29.075	0.321
8X8	1.236.699	7.931
16X16	70.025.893	451.96

4.2 Improving performance

Advantage is the fact that the matrix is sparse Haar, reduce the execution time entering in a comparison program that, when the null value is detected, the transaction between the matrices is not performed.

The Table VI presents the results comparing the values of execution time and number of operations in floating point, with and without the detection of null values.

Table VI - Comparing the values of execution time and number of operations in floating point

Divisions	Null value Execution Time (s)		Difference (%)
	Without	With	
4X4	0.321	0.250	22.12
8X8	7.931	5.488	30.80
16X16	451.96	222.60	50.75

According to the results, we can reduce 40% the time of program implementation. Figure 15 shows the values obtained for the execution time with and without the detection of null values, depending on the number of divisions of the finite plane plate.

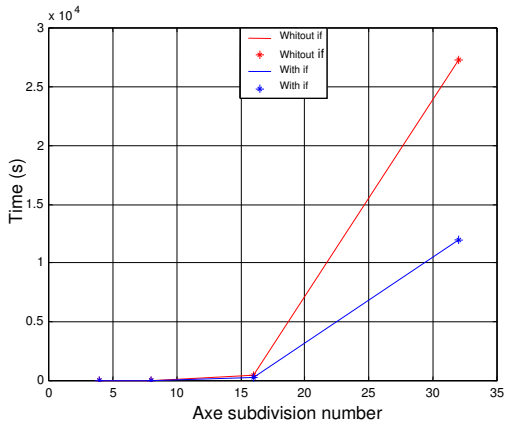

Fig. 15 - Value of execution time with and without the detection of null values

In order to briefly illustrate those aspects, one can remember that the equation to determinate the coefficients of the approximation function can be written by:

$$[Z_{mn}]*[\rho]=[V] \tag{45}$$

where, Zmn is a square matrix that is not necessarily a scattered one, since it depends on the expansion function that was chosen.

Thus, taking advantages of the fact that the Haar's matrix is a scattered matrix, applying the matrix algebra, it will result [21]:

$$[Z'_{mn}]*[\rho']=[V'] \tag{46}$$

else,

$$\begin{aligned} \left[Z'_{mn}\right] &= [H]\ \left[Z_{mn}\right]\ \left[H^T\right] \\ [\rho'] &= \left[H^T\right]^{-1}\ [\rho] \\ [V'] &= [H]\ [V] \end{aligned} \tag{47}$$

When the plate was divided into 16 equal segments in each of the axes were generated a total of 256 coefficients, with 54% of them are void. Advantage is the fact that the Haar matrix is sparse; using the algebra of matrices we can write that:

$$[H]\times[Z_{mn}]\times\left[H^T\right]\times\left[H^T\right]^{-1}\times[\rho]=[H]\times[V] \tag{48}$$

Thus, after applying such an approach, we got a symmetrical matrix. Moreover, due to the properties of Haar function a number of "near" null matrix elements were obtained.

The used approach is based on the assumption of a threshold levels. This level corresponds to a percentage of the difference between the maximum positive value and the minimum negative one: Once it is adopted, the matrix elements, inferior to this number, will be assumed as a null one. This approach will help to get an additional computing time reduction.

4.3 Improved performance with variation in threshold

Here, we show the amount of non-zero (points in blue), obtained for a plane plate with 16 division in each of the axes by selecting a threshold.

The Fig. 16 and 17 show the results obtained varying the threshold is at 0.01%, 0.05%, respectively.

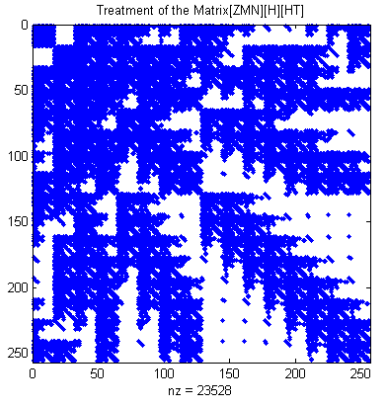

Figure 16 - Value of the threshold of 0.01% (23528 non-zero)

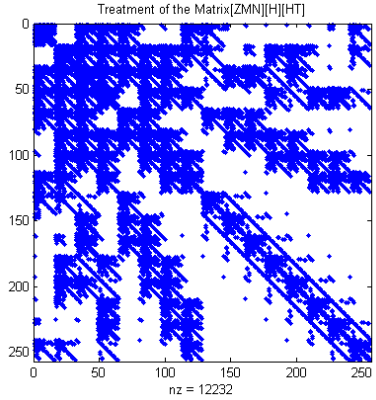

Figure 17 - Value of the threshold of 0.05% (19068 non-zero)

The Table VII shows the rate of change in percentage of the amount of non-zero when applying the threshold selected on the initial value of 65.536 points.

Table VII - Change the quantity of items in percentage depending on the threshold.

	Elements		
Threshold (%)	Quantity	Not Null (%)	Null (%)
0.00001	63.088	96.26	3.74
0.01	23.528	35.90	64.10
0.02	19.068	29.09	70.91
0.05	12.232	18.66	81.34
0.10	6.704	10.23	89.77

The Fig. 18 represents the variation of surface density of charge, for a plane plate with 16 divisions on each side, depending on the selected threshold.

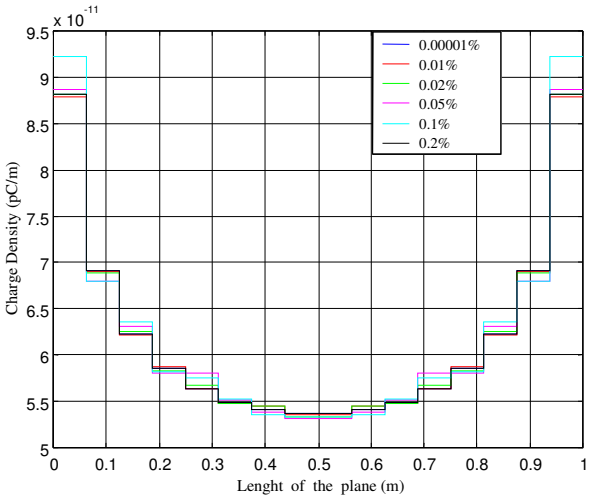

Figure 18 - Variation of surface density

The Table VIII and Fig. 19 show the variation of execution time on the solution of the system matrixes, varying the number of division of the plane plate depending on the selected threshold.

Table VIII - Execution time depending on the threshold

Division Plate	Execution Time(s)		
	0.00001%	0.05%	0.1%
16x16	0.27	0.16	0.16
32x32	25.486	4.516	2.073

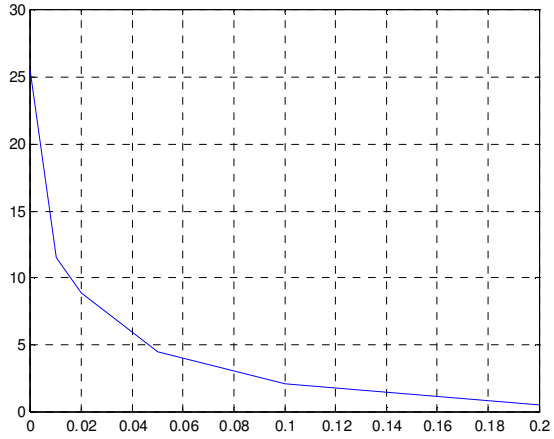

Figure 19 - Time of execution according to selected threshold

Therefore, the variation of the threshold led to a significant reduction in execution time, without significantly changing the value of the surface density of charge.

4.4 The performance using the Cholesky

An efficient method for calculating the matrix is through the decomposition of Cholesky, which considers that the matrix is symmetric positive defined [22].

Such matrices appear in a variety of applications, such as the numerical solution of initial value problems of the method of finite differences, or the method of finite elements.

A symmetrical matrix of NxN order positive is defined if X^T AX>0 for all not null vectors of x satisfying the following properties:

a) If A is a defined positive symmetrical matrix, then A is inversion;

b) If A is a defined positive symmetrical matrix, then det (A) > 0;

c) If A is a defined positive symmetrical matrix, then sub first main A_1,.....,A_n an A is all defined positive, and

d) If A is a defined positive symmetrical matrix, then A can be reduced to a superior triangular form using only elementary operations: it is inversion.

$$\begin{bmatrix} a_{11} & x & x & x \\ x & a_{22} & x & x \\ x & x & a_{33} & x \\ x & x & x & a_{44} \end{bmatrix} \rightarrow \begin{bmatrix} a_{11} & x & x & x \\ 0 & a_{22} & x & x \\ 0 & x & a_{33} & x \\ 0 & x & x & a_{44} \end{bmatrix} \rightarrow \begin{bmatrix} a_{11} & x & x & x \\ 0 & a_{22} & x & x \\ 0 & 0 & a_{33} & x \\ 0 & 0 & x & a_{44} \end{bmatrix} \rightarrow \begin{bmatrix} a_{11} & x & x & x \\ 0 & a_{22} & x & x \\ 0 & 0 & a_{33} & x \\ 0 & 0 & 0 & a_{44} \end{bmatrix} \quad (49)$$

The decomposition of Cholesky, believes that a particular order NxN matrix A can be factored into a product $A=HH^T$, where H is the lower triangular matrix with positive diagonal elements.

The matrix $A=HH^T$, also can be written in terms of a superior triangular matrix that is $R=H^T$. In fact, if $R=H^T$ then $A=HH^T = RR=H^T$.

The Fig. 20 shows the number of elements of triangular shape, obtained after the application of Cholesky with threshold of 0.01%.

$$\begin{bmatrix} a_{11} & a_{12} & \cdots & a_{1n} \\ a_{21} & a_{22} & \cdots & a_{2n} \\ \vdots & \vdots & \ddots & \vdots \\ a_{n1} & a_{n2} & \cdots & a_{nn} \end{bmatrix} = A \times B$$

$$A = \begin{bmatrix} h_{11} & 0 & \cdots & 0 \\ h_{21} & h_{22} & \cdots & 0 \\ \vdots & \vdots & \ddots & \vdots \\ h_{n1} & h_{n2} & \cdots & h_{nn} \end{bmatrix} \quad (50)$$

$$B = \begin{bmatrix} h_{11} & 0 & \cdots & h_{n1} \\ 0 & h_{22} & \cdots & h_{n2} \\ \vdots & \vdots & \ddots & \vdots \\ 0 & h_{n2} & \cdots & h_{nn} \end{bmatrix}$$

This decomposition, the partial average execution time for a plane plate with 16 divisions in each axis, changed from 0.21 to 0.02(s) and with 32 division from 11.49 in 0351(s), to further improve the overall performance of the program.

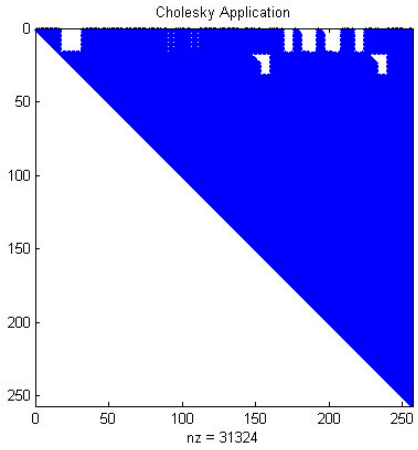

Figure 20 - Number of elements after Cholesky decomposition (0.01%)

5) Conclusion

According to the results we can observe that the numerical method presented is very efficient and accurate solutions of problems in electrostatics.

With the proposed methodology in the two cases that were the object of our study, considering the domestic product expansion of the function of the Haar wavelet function instead of the pulse (a function of the Dirac Delta weighting) and discretization of the domain of the function through points we obtained a variation in the calculation of coefficients, which contribute to the calculation of surface charge density of less than 0.025%.

Given the fact that the transformed matrix of the Haar wavelets produces sparse matrices, in alternative programming, such as the detection of null values, we obtained a decrease in the amount of floating point operations in very significant, there was a reduction in total time of the program approximately 40%.

With the selection of a threshold in percentage, which is only possible to be implemented when used as a basis for expansion of the Haar wavelet, we can eliminate some coefficients for the difference in modulus between the largest positive and less negative, we obtained an improvement in the performance of program. In the case of square plane plate with 16 divisions, in each of the axes, and a

threshold of 0.01%, achieved a reduction in execution time of 33%.

Applying the Cholesky decomposition, for a plane plate 16x16, 0.01% threshold, the average time to partial execution of the transactions between the matrixes, involved calculating the density of surface charge, reduced by approximately 10 times.

References:

[1]R. F. Harrington ,Field Computation by Moment Methods. 1.ed. New York, Macmillan Company, 1968.

[2]Constantine A. B., Advanced Engineering Eletromagnetics, 2.ed. New York, John Wiley & Sons, 1989.

[3]Cohen A., Kovacevic J. Wavelets, *The mathematical background. IEEE Proceedings of the IEEE*, v84, n.4, p.514-522, 1996.

[4]Morettin P. A. Ondas e Ondaletas, 1.ed. São Paulo, Edusp , 1999.

[5]Morettin P. A., 7° Escola de séries Temporais e Econometria, 1.ed. São Paulo, Edusp, 1997.

[6]Chui C. K., An Introduction to Wavelets. 1. Ed., Texas, Academic Press, 1992.

[7]Aboufadel, E., Schlicker S., Discovering Wavelets, 1.ed. New York, John Wiley & Sons, INC, 2000,

[8]I. Daubechies, Orthonormal bases of compactly supported wavelets, Comm. on Pure and Appl. Math. XLI, 1988, pp. 909-996

[9]Newland D. E. Random Vibrations, Spectral and Wavelet Analysis. 3.ed. Edinburgh, Addison Wesley Longman Limited, 1993.

[10]I. Daubechies, The wavelet transform, time-frequency localization and signal analysis,IEEE Trans. on Information Theory 36,1990, pp. 961-1005.

[11]S. G. Mallat, Multiresolution approximations and wavelet orthonormal bases of L2(R), Trans. Amer. Math. Soc 315 ,1989, 69-87.

[12]Benedetto J. J; Frazier M. W., Wavelets Mathematics and Applications. 1. Ed. London CRC Press, 1994.

[13]Belardi A. A, Cardoso J. R., Sartori C. F, *Application of Haar´s Wavelets in the Method of Moment to Solve Electrostatic Problems*, Poland, Instytut Maszyn Elektrycznych I Transformatorów, ISEF, 2003, pp. 15-20.

[14]Belardi A. A, Cardoso J. R., Sartori C. F., *Wavelets Application in Electrostatic and their Computing Aspects*. Germany, Electric and Magnetic Fields, EMF, 2003, pp. 43-46.

[15]Belardi A. A, Cardoso J. R., Sartori C. F., C*alculation of the Parallel Finite Plate Capacitance and the Electrical Fields using the Method of Moments and the Haar Wavelets,*Italy Electric and Magnetic Fields, EMF, 2009, pp. 43-46.

[16]Belardi A. A, Cardoso J. R., Sartori C. F., Contribuição a aplicação das wavelets na eletrostática, Brasil,2003, EPUSP.

[17]Morettin L. G. Estatística Básica (Inferência). 2.ed. São Paulo, Makron Books, 1999.

[18]Shao K. R.; Lavers J. D., Wavelet Based Multiresolution Algorithm for Integral and Boundary Element Equations in Electric and Magnetic Field Computations, IEEE Transactions and Magnetics, v38, n.5, p.2373-2375, 2002.

[19]Patterson D. A.; Hennessy J. L., Organização e Projeto de Computadores a Interface "Hardware/Software" , 1.ed. Rio de Janeiro, Livros Técnicos e Científicos - LTC, 2001

[20]Stallings W., Arquitetura e Organização de Computadores. 5.ed. São Paulo, Prentice Hall, 2002.

[21]Frazier M. W., An Introduction to Wavelets Through Linear Algebra. 1. Ed. New York, Springer, 1999.

[22]Datta B. N., Numerical Linear Algebra and Applications, 1. ed. New York, Brooks/Cole Publishing Company, 1995, pp. 222-225.